Article:
Zhang, Y, Huang, Y, Chen, H orcid.org/0000-0003-0753-7735 et al. (3 more authors) (2021) Driving behavior oriented torque demand regulation for electric vehicles with single pedal driving. Energy, 228. 120568. ISSN 0360-5442

https://doi.org/10.1016/j.energy.2021.120568

Driving Behavior Oriented Torque Demand Regulation for Electric Vehicles with Single Pedal Driving

Yuanjian Zhang[1], Yanjun Huang[2], Haibo Chen[3], Xiaoxiang Na[4], Zheng Chen[5,6*] and Yonggang Liu[7**]
[1]School of Mechanical and Aerospace Engineering, Queen's University of Belfast, BT9 5AG, Northern Ireland
[2] School of Automotive Studies, Tongji University, Shanghai, 201804, China.
[3]Institute for Transport Studies, University of Leeds, Leeds LS2 9JT, United Kingdom
[4]Department of Engineering, University of Cambridge, Trumpington Street, Cambridge CB2 1PZ, United Kingdom
[5]Faculty of Transportation Engineering, Kunming University of Science and Technology, Kunming, 650500, China
[6]School of Engineering and Materials Science, Queen Mary University of London, London, E1 4NS, United Kingdom
[7]State Key Laboratory of Mechanical Transmissions & School of Automotive Engineering, Chongqing University, Chongqing, 400044, China
Email: y.zhang@qub.ac.uk, huangyanjun404@gmail.com, h.chen@its.leeds.ac.uk, xnhn2@cam.ac.uk, chen@kust.edu.cn, andylyg@umich.edu
Corresponding Author: Zheng Chen (chen@kust.edu.cn) and Yonggang Liu (andylyg@umich.edu)
Equation Chapter 1 Section 1

Abstract: Driving behaviours, induced by psychological activities and environment stimulation, impose the dominant impact on vehicle driving performance. To exhaustively improve the performance of electric vehicles (EVs), information unscrambled from various driving behaviours is recommended to be incorporated into the controlling process. In this context, a novel method is presented to regulate the torque demand of EVs with single pedal driving (SPD) that efficiently interprets intention from different driving behaviours for eco driving. Specifically, a brand-new driving behaviour identifier (DBI) is constructed by integrally employing the binary dragonfly algorithm (BDA) and adaptive neuro-fuzzy inference system with particle swarm optimization (ANFIS-PSO). Simultaneously, the whale optimization algorithm (WOA) generates the torque demand look-up tables (TDLTs) offline under different driving behaviours for SPD by referring to the constraints from drivability and energy efficiency. In the instant implementation, the driving behaviours are identified instantaneously by the DBI, and the homologous TDLTs are assigned to vehicle controller, thereby attaining efficient control of vehicle powertrain. A case study about the vehicle traction control is performed to validate the prospective optimal performance of the proposed method and further evaluate the impact on vehicle performance from driving behaviours.

Key words: Driving behaviours, binary dragonfly algorithm (BDA), adaptive neuro-fuzzy inference system with particle swarm optimization (ANFIS-PSO), whale optimization algorithm (WOA), single pedal driving (SPD).

NOMENCLATURE

Abbreviations

EV	electric vehicle	TPD	two-pedal driving
SDP	stochastic dynamic programming	VCU	vehicle control unit
DBI	driving behavior identifier	MCU	motor control unit
BDA	binary dragonfly algorithm	PMSM	permanent magnet synchronous motor
ANFIS	adaptive neuro-fuzzy inference system	ECM	efficient equivalent circuit model
PSO	particle swarm optimization	SOC	state of charge
WOA	whale optimization algorithm	FLC	fuzzy logic control
TDLT	torque demand look-up tables	ANN	artificial neural network
HEV	hybrid electric vehicle	RMSE	root mean square error
FCEV	fuel cell electric vehicle	DA	dragonfly algorithm
RBS	regenerative braking system	GA	genetic algorithm
SPD	single pedal driving	DP	dynamic programming

Symbols

T_{mot}	torque provided by motor	$f(x)$	fitness function of ANFIS-PSO
m	vehicle mass	S	feasible space
g_{fr}	final gear efficiency	y_i	estimation value
N_{fr}	final gear ratio	$\hat{y}_i$	real value from the training data
r_w	wheel radius	X	current position of single dragonfly
ρ	air density	X_j	position of j th neighboring individual
C_d	aerodynamic drag factor	N	neighbour scale
A_d	frontal area	V_j	velocity of j th neighboring individual
v	vehicle speed	X_f	position of food source
g	gravity acceleration	X_E	position of food source
f	rolling resistant factor	s	weight for separation
θ	road gradient	a	weight for alignment
ω_{em}	angular speed of electric motor	c	weight for cohesion
P_{PMSM}	power of PMSM	f	weight for attraction
T_{PMSM}	torque of PMSM	e	weight for distraction
η_{mot}	motor efficiency in tractive mode	ω	inertia weight
η_{gen}	motor efficiency in generator mode	ΔX_{t+1}	step of next movement
T_{trac}	vehicle tractive torque	ΔX_t	step of current movement
I_{batt}	battery current	r	random value
V_{batt}	battery open circuit voltage	$\alpha ERR(D)$	classification error rate

r_{batt}	battery inner resistant	$\lvert R \rvert$	number of filtered features
P_{batt}	battery power	$\lvert N \rvert$	total number of the candidate features
SOC	battery SOC	α	complement parameters to weigh the selection error rate
Q_{batt}	battery capacity	β	complement parameters to weigh the selection error ratio
a_j	premise parameters of fuzzification	t	iteration number
b_j	premise parameters of fuzzification	$\vec{A}$	coefficient vector
c_j	premise parameters of fuzzification	$\vec{C}$	coefficient vector
I_1	mentioned inputs	$\overrightarrow{X^*}$	best solution position
I_2	mentioned inputs	$\vec{X}$	position vector
μ_{A_j}	membership function	$\vec{a}$	vector that linearly decreases from 2 to 0 with the iteration going
O_j^1	output of fuzzification layer	$\vec{r}$	random vector in [0, 1]
p_j	consequent parameter of defuzzification	$\overrightarrow{D'}$	distance of certain to the current best solution
q_j	consequent parameter of defuzzification	b	constant value to formulate profile of the spiral path
r_j	consequent parameter of defuzzification	l	a random number in [-1, 1]
$X_{i,n}$	position of the i th particle at n th iteration	p	random value in [0, 1]
$V_{i,n}$	velocity of the i th particle at n th iteration	$\overrightarrow{X_{rand}}$	random chosen position vector from current population
j	dimension space	X	search agent that represents solutions of the optimization problem
c_1	acceleration coefficient	$\dot{m}_{ress}$	velocity resulted from solutions in current step
c_2	acceleration coefficient	v	reference velocity from the given driving cycle
φ	uniformly distributed random variable	V_{ref}	penalty matrixes in MPC based optimal tracking
ψ	uniformly distributed random variable	ϑ_1	weight ratio
$P_{i,n}$	personal best position	ϑ_2	weight ratio
G_n	global best position		

I. INTRODUCTION

Electrified transportation has made significant contribution to environment protection, global warming mitigation and energy consumption structure adjustment [1, 2]. A large amount of validated solutions have emerged in the evolution of electrification, including electric vehicles (EVs) [3], hybrid electric vehicles (HEVs) [4] and fuel cell electric vehicles (FCEVs) [5]. To fully advance the potential of these outstanding solutions in energy saving, key control techniques [6, 7] in these solutions deserve to be carefully investigated. For EVs, driving requirement is usually regulated by the torque demand look-up tables (TDLTs), which mainly account for translating the driving intention into torque requirement of electric powertrains and are rather critical for efficient driving. To attain the full-state eco-driving, it is quite recommended to develop a novel method that can generate efficient TDLTs under different driving behaviours, so as to optimally regulate the toque demand with the strengthened energy-efficiency for EVs. To fully promote the capacity of electrified transportation in energy saving, researches on key technologies have gained promising progress. Aiming to properly manage power flow within hybrid powertrain, a variety of control strategies have been spurred, including rule based strategies [8, 9], global optimization based strategies [10, 11], instantaneous optimization based strategies [12, 13], and machine learning based strategies [14, 15]. All the methods declare to lead to massive advantages in improving energy-efficiency under certain conditions. On the other hand, the capability of fully recycling braking energy is one notable preponderance in electrified transportation. To maximize the recycling of regenerative braking energy without scarifying drivability and safety, some well-designed regenerative braking systems (RBSs) have been devised [16], and the fully- and partially-coupled solutions are widely adopted [17]. In addition, full consideration of driving behaviours can contribute to promotion of energy economy, and similarly eco driving assistant systems were developed in past years to educate driving vehicles with eco-friendly manners and partial interpretation of driving behaviours [18, 19].

Among the promising key techniques for energy saving, single pedal driving (SPD) [20] is one innovative solution for EVs. The SPD cannot only bridge driving behaviours with vehicle plants, but also imitate engine braking in EVs during the cruise stage and maximize the recycled braking energy in urban roads [21]. Currently, studies on SPD have been progressively advanced. The methods to maximize regenerative braking energy in EVs with SPD is proposed in [22] for energy economy promotion of EVs. The introduction of SPD might alter the driving manners, probably discounting driving safety and driving comfort. Some related studies have been

performed to guarantee driving safety and prompt driving comfort. Ref. [23] presents a joint method to successfully improve driving safety of SPD in EVs under multiple constraints. Ref. [24] investigates the performance of haptic pedal feel compensation for improving driving comfort of SPD. The experimental results indicate that the haptic pedal feel compensation can minimize the solid braking instance and smooth the driving comfort evidently. Similar with traditional two-pedal driving (TPD), manoeuvres of drivers on acceleration pedals in SPD are also transformed into driving torques by TDLTs. Driving intentions resulted from different behaviours are conveyed to vehicle via pedals in SPD and TPD, and will affect energy consumption after incorporation of the specific torque demand obtained by TDLTs. The close coupling between driving behaviours and energy consumption suggests the study on torque demand regulation in EVs with SPD for efficient driving after integrating driving behaviours. The torque demand regulation for EVs with SPD integrates driving behaviours analysis, to the best of authors' knowledge, is rarely investigated. Actually, most of the existing solutions to regulate the torque demand of EVs with SPD belong to rule based methods [25]. By applying the well-designed deterministic rules [26] or fuzzy rules [27], the torque demand is optimized for EVs with SPD to maximize energy utilization efficiency without influencing drivability. In [28], specific torque demand regulation is conducted by means of an exquisitely devised fuzzy controller which outputs appropriate regenerative braking torques generated by acceleration pedal, thereby reducing electricity during eco-driving. While, rule based methods are difficult to further improve the performance of torque demand regulation, and instead optimization theories, which, up to now, are seldom applied in torque regulation of EVs with SPD, may supply an alternate manner to attain the promotion.

It is known that driving behaviours show massive influence on vehicle performance in different perspectives. The driving behaviours express psychological activities of drivers after receiving stimulations from environment [29]. In recent years, studies on driving behaviour analysis have continuously emerged, mainly including driving behaviour generation and driving style classification. In the fields related to driving behaviour generation, qualitative and quantitative analysis methods have been widely employed to uncover the factors that may cause and alter driving behaviours [30, 31]. Driving behaviour classification is tightly connected with human-machine driving in autonomous vehicles [32, 33]. Machine learning methods [34] and deep learning algorithms [35] have been proposed to efficiently identify different driving behaviours. Despite

the satisfying achievement, driving behaviour analysis in studies related to torque demand regulation in EV with SPD is still located in its preliminary stage.

According to the literature review, EVs with SPD raise massive potential in eco-driving, of which the torque demand regulation can be exquisitely conducted under different driving behaviours. After minutely studying the state-of-the-art methods related to identification and application of driving behaviours, a novel torque demand regulation method, with the integration of driving behaviour identification, is proposed for EV with SPD to attain eco-driving under different driving behaviours. To be specific, an efficient driving behaviour identifier (DBI) is firstly constructed, wherein the adaptive neuro-fuzzy inference system with particle swarm optimization (ANFIS-PSO) classifies driving behaviours on the basis of inputs that are selected by the binary dragonfly algorithm (BDA). Then, a novel torque demand regulation method is raised to achieve eco-driving. By referring to the classified driving behaviours, the customized TDLTs for different driving behaviours are generated offline by the whale optimization algorithm (WOA). In practical implementations, the generated TDLTs for various driving behaviours, together with the novel DBI, are programmed into vehicle control unit (VCU). The DBI identifies driving behaviour instantaneously, and VCU calculates the required tractive torque accordingly based on the specific TDLT corresponding to the classified driving behaviour. Four main contributions highlighting the research importance are added to the existing literature, and can be summarized as:

1) A novel driving behaviour-oriented torque demand regulation method is proposed for EV with SPD. By optimally regulating the torque demand under disperse driving behaviours, the eco-driving potential of the studied EV with SPD can be further advanced.
2) An efficient DBI is constructed in the novel torque demand regulation method to effectively categorize driving behaviours in real-time implementation. To promote classification accuracy, the ANFIS-PSO and BDA are integrally employed in DBI construction. The BDA selects the valuable input features among the transferred signals as the inputs of ANFIS-PSO algorithm.
3) The WOA is exploited in the novel torque demand regulation method to optimally generate TDLTs for eco-driving under various driving behaviours.

4) A case study in terms of optimal traction control for EV with SPD is performed to validate the superior performance of the raised torque demand regulation method, and further address the essential role of driving behaviours under efficient driving conditions.

The remainder of this paper is organized as follows. The studied EV and related model construction are described in Section II. The designed torque demand regulation method, incorporating DBI design and TDLTs generation is elaborated in Section III, and Section IV introduces the identification results and details the case study. The main conclusions are drawn in Section VI.

II. EV MODEL CONSTRUCTION

2.1 The Studied EV and SPD Function

In EVs, VCU receives driving commands from driver and calculates the required tractive torque through interpolating TDLTs. The calculated tractive torque is converted into the load rate and then transmitted to motor control unit (MCU). In this paper, the detailed parameters of studied EV is listed in Table 1.

Table 1 Main parameters of EV

Item	**Variable**	**Values**
Vehicle	Vehicle Mass	1552 kg
	Wheel Radius	0.307 cm
	aerodynamic drag coefficient	0.28
Battery	Type	Lithium-ion battery
	Capacity	60 Ah
	Nominal Voltage	330 V
Motor	Maximum Power	90 kW
	Maximum Torque	300 Nm
Performance	Max Speed	160km/h
	Max Travel Mileage	170 km

In the studied EV, SPD enables driver to manipulate the powertrain by a single pedal, avoiding frequently operating brake pedal in city urban driving and consequently maximizing the regenerated braking energy. The brief illustration of the SPD function is shown in Fig. 1.

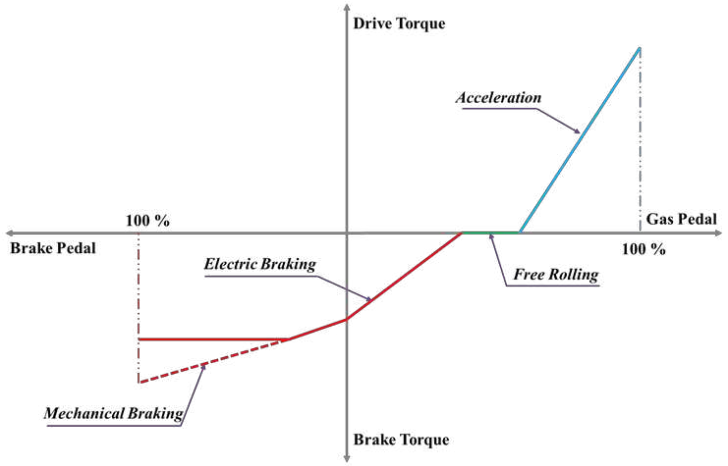

Fig. 1. Illustration on SPD.

As shown in Fig. 1, the driver can manipulate the acceleration pedal to realize braking in SPD when releasing the acceleration pedal lower than a pre-set threshold. Between acceleration phase and braking phase, a free rolling mode is designed in SPD, trying to exhausting the available kinetic energy. In the braking phase in SPD, only motor provides the braking force. When the braking process is taken over by the braking pedal, the braking force will be distributed between the hydraulic resistance and electric regenerative braking. In next step, EV model, accounting for vehicle dynamic and powertrain performance, is addressed to facilitate the design of the proposed torque demand regulation method.

2.2 Vehicle Dynamic Model

Vehicle models, including backward and forward manners, play an essential role in control strategy development. The backward models are more convenient for energy estimation [36]. In these approaches, the calculation is initiated from wheels, and then the required driving torques are decomposed into different energy paths through the transmission system [37]. By contrast, the forward modelling approach starts simulation from the driver module [38]. The control units process driving intention, and the corresponding control commands are generated and transmitted to power units. The intuitive forward calculation manner makes it widely accepted in development of modern vehicle control systems [39]. However, considering the specific features of TDLT optimization, the backward modelling manner is preferred in this study. The adopted EV is driven by a single permanent magnet synchronous motor (PMSM) installed in front axle. The torque generated by PMSM is transmitted to wheels via the final gear. The following function can be formulated to characterize the vehicle dynamics, as:

$$\begin{aligned}\dot{v}(k) &= \frac{1}{m}\left(\frac{g_{fr}N_{fr}}{r_w}T_{mot}(k) - \frac{1}{2}\rho C_d A_d v(k)^2 - mgf\cos\theta(k) - mg\sin\theta(k) - \frac{T_{brk}}{r_w}\right) \\ &= \frac{1}{m}\left(P_1 T_{mot}(k) - P_2 v(k)^2 - P_3 - \frac{T_{brk}}{r_w}\right)\end{aligned} \tag{1}$$

where $P_1 = g_{fr}N_{fr}/r_w$, $P_2 = \frac{1}{2}\rho C_d A_d$, and $P_3 = mgfcos\theta(k) + mgsin\theta(k)$. In (1), T_{mot} means the torque provided by the motor; m, g_{fr}, N_{fr} and r_w express the vehicle mass, final gear efficiency, final gear ratio, and wheel radius; ρ, C_d, A_d and v represent the air density, aerodynamic drag factor, frontal area, and vehicle speed; g, f and θ indicate the gravity acceleration, rolling resistant factor, and road gradient; and T_{brk} is the mechanical braking torque.

2.3 Vehicle Powertrain Model

2.3.1 Motor Model

In EV, PMSM is the only tractive source, of which the performance significantly determines the whole vehicle dynamics. In torque demand regulation studies, it is imperative to carefully construct the PMSM model that can describe its key features and bridge vehicle behaviours with energy consumption. Accordingly, the relationships between PMSM torque and power as well as between PMSM torque and vehicle tractive torque should be clarified in the model. As such, the equations should be built to describe torque and power connection of PMSM, and also characterize the PMSM torque and vehicle tractive torque performance. Considering the main target and operation complexity in this paper, the dynamic behaviours and temperature features of PMSM are neglected. The PMSM can operate in both tractive or generator mode, and the relationship to describe motor performance can be formulated, as:

$$P_{PMSM} = \begin{cases} \dfrac{T_{PMSM}\omega_{em}}{\eta_{mot}} & T_{PMSM} > 0 \\ T_{PMSM}\omega_{em}\eta_{gen} & T_{PMSM} \le 0 \end{cases} \tag{2}$$

where ω_{em} is the angular speed of electric motor; P_{PMSM} and T_{PMSM} denote the power and torque of PMSM; and η_{mot} and η_{gen} are the efficiency of PMSM in tractive mode and generator mode, respectively. The efficiency of PMSM can be located from the look-up table obtained through benchmark test. In the nonlinear optimization, interpolating the efficiency look-up table step by step may increase the computation intensity,

and improper interpolation may lead to undesired optimization results. To guarantee the application effect, it is suggested to utilize a multi-order polynomial function to approximate the efficiency look-up table. To simplify the process of optimal design, the look-up table for PMSM operation efficiency is approximated by a multi-order polynomial function, whose performance is depicted in Fig. 2. By considering the fitting accuracy and processing complexity, a five-order polynomial function is exploited to achieve the approximation. Accordingly, the three-dimension (3D) efficiency map of PMSM can be reformulated, as:

$$P_{mot}=\begin{cases}\eta_{mot}=a+bm(x,y)+cm^2(x,y)+dm^3(x,y)+em^4(x,y)+fm^5(x,y)\\ m(x,y)=a_{10}x+a_{01}y+a_{11}xy\\ m^2(x,y)=a_{20}x^2+a_{02}y^2+a_{21}x^2y+a_{12}xy^2+a_{22}x^2y^2\\ m^3(x,y)=a_{30}x^3+a_{03}y^3+a_{31}x^3y+a_{13}xy^3+a_{32}x^3y^2+a_{23}x^2y^3\\ m^4(x,y)=a_{40}x^4+a_{04}y^4+a_{41}x^4y+a_{14}xy^4\\ m^5(x,y)=a_{50}x^5+a_{05}y^5\end{cases} \tag{3}$$

where x means the motor speed ω_{em}, and y expresses the motor torque T_{mot}. The parameters in (3) are estimated by the particle filter method detailed in [40]. During identification, the parameters are updated in each iteration by importance sampling according to the Bayes' theorem, until the root means square error (RMSE) between the five-order polynomial function and look-up table is less than the pre-set value. Fig. 2 depicts the approximation effect by the five-order polynomial function.

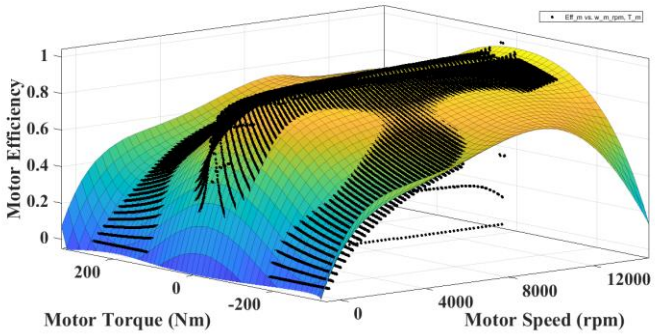

Fig. 2. Motor map with the simplified approximation by polynomial function.

Moreover, the relationship between PMSM torque and tractive torque can be formulated, as:

$$T_{PMSM}=\begin{cases}\dfrac{T_{trac}}{\eta_{mot}N_{fr}} & T_{trac}>0\\ T_{trac}N_{fr}\eta_{gen} & T_{trac}\le 0\end{cases} \tag{4}$$

where T_{trac} is the vehicle tractive torque.

2.3.2 Battery Model

For ease of modelling the battery, the temperature influence and aging effect are neglected, and a simple but efficient equivalent circuit model (ECM) is employed to characterize the battery's electrical performance. The model consists of an internal resistance and an open circuit voltage source connected in series, whereupon the battery current can be calculated, as:

$$I_{batt} = \frac{V_{batt} - \sqrt{V_{batt}^2 - 4r_{batt}P_{batt}}}{2r_{batt}} \tag{5}$$

where I_{batt} and V_{batt} denote the battery current and open circuit voltage; r_{batt} and P_{batt} are the battery inner resistance and power, respectively. The battery state of charge (SOC) can be calculated by:

$$\dot{SOC} = -\frac{V_{batt} - \sqrt{V_{batt}^2 - 4r_{batt}P_{batt}}}{2r_{batt}Q_{batt}} \tag{6}$$

where SOC is the battery SOC, and Q_{batt} is the battery capacity.

III. Development of the Novel Torque Demand Regulation Method

The novel torque demand regulation method aims to realize eco-driving under all conditions without discounting drivability by generating and implementing TDLTs that are corresponding to different driving behaviors. The novel torque demand regulation method is fulfilled via the cooperation between offline optimization and online adaptive control. In instant adaptive implementation, VCU selects a certain refined TDLT according to the driving behavior identified by the novel DBI. Then, based on the acceleration pedal degree, VCU calculates the required traction torque, which will be transmitted to MCU to order the operation of PMSM accordingly. The novel DBI is developed based on the ANFIS-PSO algorithm, which possesses high-quality performance in driving behavior categorization after proper training. The classified driving behaviors include three types: Expert Pro, Normal and Eco Pro. To strengthen the performance of the novel DBI, the inputs of ANFIS-PSO based DBI are rationally filtered by BDA among a number of vehicle signals, that are highly connected with driving behaviors. The offline implementing process of the novel torque demand regulation method is mainly related to the optimal generation of TDLTs. WOA, as one of the latest multi-objective optimization algorithms, is exploited to create TDLTs for time-varying driving behaviors. Here, the construction of TDLTs fully considers the characteristics of three driving behaviors, the target of eco-driving, and constraints of drivability. Additionally, the input selection for ANFIS-PSO based DBI and the training of DBI are also achieved in offline implementation.

The general implementation of the novel torque demand regulation method is sketched in Fig. 3. As can be found, there exists three driving modes, namely Expert Pro, Normal and ECO Pro. In terms of Expert Pro mode, drivers tend to drive vehicles aggressively with higher energy consumption. For Eco Pro mode, drivers manipulate vehicles moderately to save energy utilization while keeping safety. Divers with Normal behaviors attempt to achieve the trade-off balance between energy-efficiency and drivability. In following sections, the methods to classify driving behaviors and generate TDLTs will be detailed.

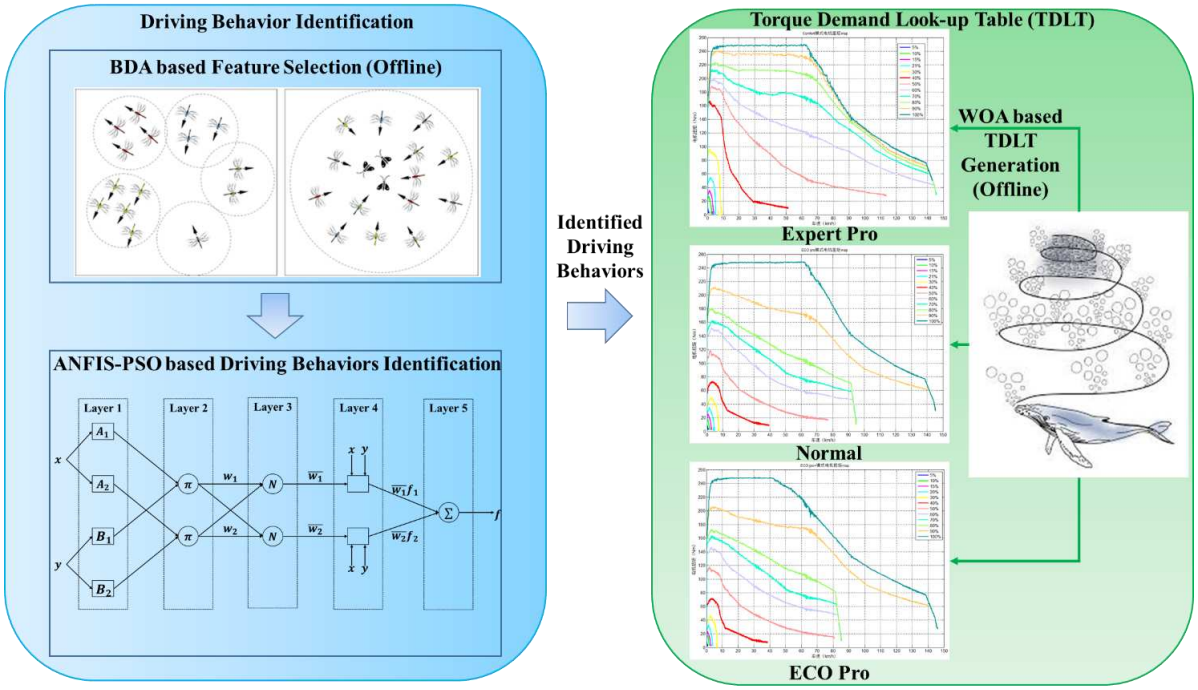

Fig. 3. Novel driving-behaviours-oriented torque demand regulation method.

3.1 Novel Driving Behaviors Identifier

3.1.1 Enhanced Adaptive Neuro-Fuzzy Inference System Based Driving Behavior Identification

The adaptive neuro-fuzzy inference system (ANFIS) is an intelligent fusion method by comprehensively exploiting the merits of fuzzy logic control (FLC) and artificial neural network (ANN), thus intelligently prompting the modelling process of complex problem [41]. Fig. 4 illustrates the general framework of ANFIS, which includes two inputs and one output. Normally, there are five layers in ANFIS to accomplish the input-output mapping. The detailed transformation and calculation can be described as follows.

Layer 1 (Fuzzification): The fuzzification is performed in this layer by using the membership function, as:

$$\mu(x)=\frac{1}{1+\left[\left(\left(x-c_j\right)/a_j^2\right)\right]^{b_j}} \quad j=1,2 \tag{7}$$

where a_j, b_j and c_j are the premise parameters. Accordingly, the output of Layer 1 can be formulated, as:

$$\begin{cases} O_j^1 = \mu_{A_j}(I_1) & j = 1,2 \\ O_j^1 = \mu_{B_j}(I_1) & j = 1,2 \end{cases} \tag{8}$$

where I_1 and I_2 are the two mentioned inputs, μ_{A_j} is the membership function, and O_j^1 is the output of this layer.

Layer 2 (Product): The firing strength of Sugeno-fuzzy rules is calculated by a multiple operator, as:

$$O_j^2 = w_j = \mu_{A_j}(I_1) \cdot \mu_{B_j}(I_2) \quad j = 1,2 \tag{9}$$

Layer 3 (Normalized): The firing strength of a give rule is normalized in this layer by:

$$O_j^3 = \overline{W_J} = \frac{w_j}{w_1 + w_2} \quad j = 1,2 \tag{10}$$

Layer 4 (Defuzzification): The weighted consequent value of each rule is calculated based on the normalized firing strength in upper layer, as:

$$O_j^4 = \overline{W_I} Z_i = \overline{W_I}(p_j I_1 + q_j I_2 + r_j) \tag{11}$$

where p_j, q_j and r_j are the consequent parameter.

Layer 5 (Output): The overall output, corresponding to all inputs, can be calculated as:

$$O_j^5 = \sum_j \overline{W_I} Z_i \tag{12}$$

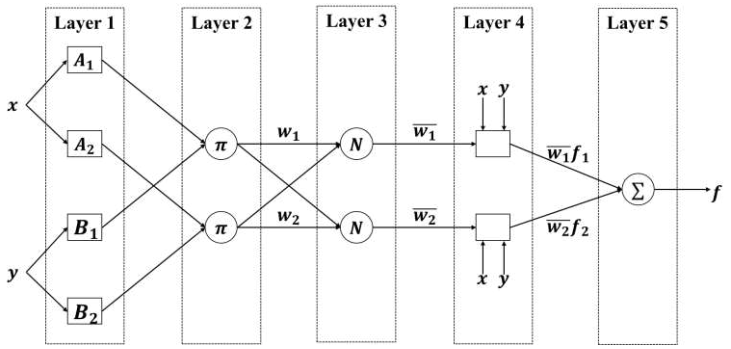

Fig. 4. General framework of ANFIS.

In this study, an enhanced ANFIS, ANFIS-PSO, is preferred to improve the accuracy of ANFIS in DBI. As the name implies, the particle swarm optimization (PSO) is integrated into the ANFIS to optimize the number of membership functions and the parameters in them. To be specific, ANFIS is firstly normally trained via the supervised learning. During this training, a fusion learning algorithm, combining the gradient decent

method [42] and least square method [43], identifies the premise parameters and the remaining parameters. Then, the mentioned target is optimized by the PSO, in which RMSE is considered as the fitness value. By referring to the first step, the premise parameters are estimated by the gradient method, while the least square method determines the consequent parameters. In the forward training process, the least square method captures the consequent parameters while keeping the premised parameters fixed. Then, the error between predicted values and raw data is propagated backward. The least square method identifies the premise parameters by minimizing the quadratic cost function. During backward propagation, the consequent parameters remain unchanged. The PSO is one of swarm intelligence methods that globally searches the optimal solutions [44]. In PSO based optimization, the particles that represent the problem solutions try to approximate the optimal ones by updating the position and flying velocity in each iteration. The position and flying velocity of each particle can be formulated as:

$$\begin{cases} X_{i,n} = (X_{i,n}^1, X_{i,n}^2, \ldots X_{i,n}^N) \\ V_{i,n} = (V_{i,n}^1, V_{i,n}^2, \ldots V_{i,n}^N) \end{cases} \tag{13}$$

where $X_{i,n}$ and $V_{i,n}$ denote the position and velocity of the ith particle $(1 \le i \le M)$ at nth $(1 \le n \le N)$ iteration. The manners to update position and velocity can be defined, as:

$$\begin{cases} V_{i,n+1}^j = V_{i,n}^j + c_1 \varphi_{i,n}^j (P_{i,n}^j - X_{i,n}^j) + c_2 \psi_{i,n}^j (G_n^j - X_{i,n}^j) \\ X_{i,n+1}^j = X_{i,n}^j + V_{i,n+1}^j \end{cases} \tag{14}$$

where $j = 1, 2, \ldots, N$ denotes the dimension space, c_1 and c_2 are the acceleration coefficients, φ and ψ are the uniformly distributed random variables, $P_{i,n}$ is the personal best position, and G_n is the global best position. The general optimization problem by PSO can be described, as:

$$Minf(x), s.t.\ X \in S \subseteq R^N \tag{15}$$

where $f(x)$ is the fitness function to evaluate the effect of each iteration, and S denotes the feasible space. The fitness function in PSO for ANFIS is designed to achieve the lower error in prediction, as:

$$f(x) = \sqrt{\frac{1}{m} \sum_{i-1}^{m} (y_i - \hat{y}_i)^2} \tag{16}$$

where y_i is the estimation value, and $\hat{y}_i$ is the real value from the training data. As described in (7) to (12), the complexity of ANFIS can increase remarkably with more input features. To guarantee the effectiveness in

instant application, the input features of ANFIS-PSO based DBI need to be selected properly. An efficient method, BDA, is preferred to accomplish the feature selection for ANFIS-PSO based DBI. In addition, the method that clusters driving behaviors into Expert Pro, Normal and Eco Pro is the same with that in our former work [45].

3.1.2 Binary Dragonfly Algorithm Based Feature Selection

Dragonfly algorithm (DA) is one of bio-inspired algorithm for optimization problem, and can approximate the static and dynamic swarm behaviors of dragonflies in nature [46]. Among dragonflies, hunting and migration are two main swarm behaviors that are similar to exploitation and exploration in metaheuristic search. On this account, DA is considered to be an efficient tool to search the optimal solutions by the swarming intelligent manner.

A. The Basis for Feature Selection: DA

In nature, dragonflies generally employ five actions to accomplish hunting and migration, inducing the development of corresponding operator in DA [47]. The mentioned five actions consist of separation, alignment, cohesion, attraction and distraction. Accordingly, the inspiringly designed operators in DA can be characterized, as:

- Separation means that the individual dragonfly moves in the swarm without colliding surrounding individuals, and can be formulated as:

$$S_i = -\sum_{j=1}^{N} X - X_j \tag{17}$$

where X denotes current position of single dragonfly, X_j means the position of the j th neighbouring individual, and N is neighbour scale.

- Alignment refers to the single dragonfly that adjusts the flying velocity based on the movement behaviors of neighbor. The adapting behavior can be expressed, as:

$$A_i = \frac{\sum_{j=1}^{N} V_j}{N} \tag{18}$$

where V_j represents the velocity of j th neighbouring individual.

- Cohesion means that the preference of individual dragonfly towards neighbouring the center of mass. The mathematical equation in terms of model cohesion behaviour can be presented, as:

$$C_i = \frac{\sum_{j=1}^{N} V_j}{N} - X \tag{19}$$

- Attraction indicates the attractive degree between food source and individual dragonfly, as:

$$F_i = X_f - X \tag{20}$$

where X_f is the position of food source.

- Distraction presents the repulsive degree between enemy and individual dragonfly, as:

$$E_i = X_E - X \tag{21}$$

where X_E is the position of food source.

Similar with the position updating mechanism in PSO, DA also employs two vectors, i.e., step and position, to update the status of single dragonfly. The step vector of next movement is defined, as:

$$\Delta X_{t+1} = \left(sS_i + aA_i + cC_i + fF_i + eE_i \right) + \omega \Delta X_t \tag{22}$$

where s, a, c, f and e denote the weights for separation, alignment, cohesion, attraction and distraction; ω means the inertia weight; ΔX_{t+1} and ΔX_t express the step of next movement and current movement. The position of one dragonfly can be described, as:

$$X_{t+1} = X_t + \Delta X_{t+1} \tag{23}$$

B. Binary Dragonfly Algorithm for Feature Selection

The feature selection, briefly, is a binary optimization problem, in which the individual location is determined by the discrete position vector. However, DA originally focuses on continuous optimization problems, demanding some improvement for feature selection in discrete domain. Consequently, BDA is developed to promote feature selection [48]. In BDA, the position updating manners are reconstructed, as:

$$X_{t+1} = \begin{cases} X_t & r < T(\Delta x_{t+1}) \\ X_t & r \geq T(\Delta x_{t+1}) \end{cases} \tag{24}$$

where r is the random value between 0 and 1. $T(\Delta x_{t+1})$ can be calculated, as:

$$T(\Delta x_{t+1}) = \frac{|\Delta x|}{\left| \sqrt{(\Delta x^2) + 1} \right|} \tag{25}$$

Table 2 presents the pseudocode of BDA algorithm. During the feature selection process, the solutions are represented by [0, 1], where "0" indicates that the certain feature shows less connection with the predefined performance, while "1" expresses that a specific feature is selected with positive relationship with the given index. In this paper, the feature selection is attained by BDA with the wrapper selection manner. The particular fitness function, considering classification error and selection error, can be formulated as:

$$Fitness = \alpha ERR(D) + \beta \frac{|R|}{|N|} \tag{26}$$

where $\alpha ERR(D)$ is the classification error rate by using the k-Nearest Neighbor (KNN) classifier, $|R|$ is the number of filtered features, $|N|$ is the total number of the candidate features, α and β are the complement parameters to weigh the selection error rate and ratio.

Table 2. The pseudocode of BDA.

1	**Initialization: randomly define population and step vector**
2	**Do {**
3	Evaluate each dragonfly by fitness function
4	Update s, a, c, f, e and w
5	Calculate S, A, C, and F by (17) to(21)
6	Update step vector by (22)
7	Calculate $T(\Delta x_{t+1})$ by (25)
8	Update position of each dragonfly by (24)
	$q = q + 1$
9	**} Until** $q = N_i$ (N_i denotes the iteration times)

The valuable features for ANFIS-PSO based DBI is selected by the BDA among 80 signals from EV powertrain and plant, including acceleration pedal degree, steer wheel angle, etc. The data for feature selection are the same with that for DBI training. By applying the BDA, the selected features as the inputs of ANFIS-PSO based DBI can be: acceleration pedal degree, variation rate of acceleration pedal degree, braking pedal degree, variation rate of braking pedal degree, steer wheel angle and angle variation rate of steer wheel. The output of ANFIS-PSO based DBI is one specific driving behavior type that is selected from Expert Pro, Normal and Eco Pro. The training data for ANFIS-PSO based DBI is prepared in advance by the same method described in [45]. According to the selected inputs by BDA, the specific ANFIS-PSO based DBI can be constructed, and the detailed parameters of the built ANFIS-PSO based DBI are listed in Table 3.

Table 3. The parameters of the ANFIS-PSO based DBI.

Number of Inputs	6
Number of Membership Functions for Each Inputs	2
Number of Particle for Each Population	24

Epoch of Each Population	100

3.2 Torque Demand Look-up Table Generation

3.2.1 Whale Optimization Algorithm Based Optimization

WOA is one of the novel meta-heuristics optimization methods inspired from hunting behaviors of humpback whales [49]. During hunting, humpback whales adopt specific manners, which include random scan, encircling and bubble-net attacking, thus inspiring the imitation in the convergence process during optimization [50]. Due to this, WOA is introduced to be applied in complex optimization. Compared with existing optimization methods, e.g. genetic algorithm (GA) [51], WOA can show better balance between exploration and exploitation, thereby avoiding from being trapped into local optimum and achieving faster convergence.

A. Exploitation (*Encircling and Bubble-Net Attacking*)

Humpback whales encircle prey after observing its location. Accordingly, WOA assumes that the current best candidate solution is the prey, and lets searching agents update positions towards the assumed best solution. This encircling behavior can be modelled, as:

$$\vec{D} = \left| \vec{C} \cdot \overrightarrow{X^*}(t) - \vec{X}(t) \right| \tag{27}$$

$$\vec{X}(t+1) = \overrightarrow{X^*}(t) - \vec{A} \cdot \vec{D} \tag{28}$$

where t is the iteration number, $\vec{A}$ and $\vec{C}$ are the coefficient vectors, $\overrightarrow{X^*}$ is the best solution position that is updated in each iteration, and $\vec{X}$ is the position vector. The coefficients vectors in (27) and (28) can be calculated, as:

$$\begin{cases} \vec{A} = 2\vec{a} \cdot \vec{r} - \vec{a} \\ \vec{C} = 2\vec{r} \end{cases} \tag{29}$$

where $\vec{a}$ represents a vector that linearly decreases from 2 to 0 with the iteration, $\vec{r}$ is the random vector in [0, 1]. Eqn. (28) permits to search any position in the allowed space around the current best position, simulating the process of encircling prey. Bubble-net attacking by humpback whales spirits a novel exploitation method for meta-heuristics optimization. During bubble-net attacking, two actions are executed including shrinking

encircling and spiral moving. The mathematic models to demonstrate the two behaviors in bubble-net attacking can be described as follows.

1. Shrinking encircling. The shrinking encircling can be realized by linearly reducing $\vec{a}$ from 2 to 0 in different iterations. By assigning random values for $\vec{A}$ in [-1, 1], the shrinking encircling can define the new position of a search agent between the original one and current best value.

2. Spiral moving. When hunting the prey, the path of humpback whales to the identified prey is a helix shape. The spiral movement can be expressed, as:

$$\vec{X}(t+1) = \overrightarrow{D'} \cdot e^{bl} \cdot \cos(2\pi l) + \overrightarrow{x^*}(t) \tag{30}$$

where $\overrightarrow{D'}$ expresses the distance of certain to the current best solution (prey), b denotes the constant value to formulate profile of the spiral path, l means a random number in [-1, 1]. In (30), $\overrightarrow{D'}$ can be calculated, as:

$$\overrightarrow{D'} = \left| \overrightarrow{x^*}(t) - \vec{X}(t) \right| \tag{31}$$

During the prey, the humpback whales encircle the prey and swim towards the prey along the spiral path simultaneously. We can assume that each behaviour is chosen with 50% probability. Hence, the overall mathematic model to describe the exploitation phase can be expressed, as:

$$\vec{X}(t+1) = \begin{cases} \overrightarrow{X^*}(t) - \vec{A} \cdot \vec{D} & p < 0.5 \\ \overrightarrow{D'} \cdot e^{bl} \cdot \cos(2\pi l) + \overrightarrow{x^*}(t) & p > 0.5 \end{cases} \tag{32}$$

where p is the random value in [0, 1].

B. Exploration (*Prey Search*)

Except encircling and attacking prey, the humpback whales also search prey randomly in the allowed space based on the position of each other. $\vec{A}$ is utilized to direct the prey searching in exploration phase, and its value is supposed to be larger than 1 or smaller than -1. Here, it is assumed that exploration is activated if $\left|\vec{A}\right| > 1$, enforcing the global searching to avoid local optimum. The equations to model the exploration can be formulated, as:

$$\vec{D} = \left| \vec{C} \cdot \overrightarrow{X_{rand}}(t) - \vec{X}(t) \right| \tag{33}$$

$$\vec{X}(t+1) = \overrightarrow{X_{rand}}(t) - \vec{A} \cdot \vec{D} \tag{34}$$

where $\overrightarrow{X_{rand}}$ is the random chosen position vector from current population. The pseudocode of WOA is shown in Table 4.

Table 4. The pseudocode of WOA.

```
Initialization: Randomly define whale population Xi (i=1,2,…,n)
                Calculate the fitness value of each search agent
                Obtain best search agent X*
Do {
    for i=1:n
     Update a, A, C, l and p
       if p<0.5
          if |A|<1
             Update the position of current search agent by (27)
          else if |A|≥1
             Select a random search agent Xrand
             Update the position of current search agent by (34)
          end
       else if p≥0.5
             Update the position of current search agent by (30)
       end
    end
    Calculate the fitness value of each search agent
    Update X* if there is a better solution
} Until t = Ni  ( Ni : maximum number of iteration)
Return X*
```

3.2.2 Torque Demand Look-up Table Generation by Whale Optimization Algorithm

In WOA based TDLT generation, the fitness function evaluating the solution in each iteration can be formulated by considering constraints from energy-efficiency and drivability, as:

$$f(x) = \sum \vartheta_1 \dot{m}_{ress}(X) + \vartheta_2 \left(v(X) - V_{ref}(X) \right)^2 \tag{35}$$

where X is the search agent that represents solutions of the optimization problem, $\dot{m}_{ress}$ is the equivalent fuel consumption converted from the electric energy utilization, v denotes the velocity resulted from solutions in current step, V_{ref} is the reference velocity from the given driving cycle that is specifically for certain driving behaviour, and ϑ_1 and ϑ_2 denote the weight ratios. During TDLT generation, the optimized parameters include torques corresponding to different acceleration pedal degrees and velocities. To generate TDLTs for various driving behaviours, ϑ_1 and ϑ_2 are tuned accordingly during the optimization. The equivalent fuel consumption can be calculated, as:

$$\dot{m}_{ress} = \frac{s}{Q_{lhv}} P_{batt} \tag{36}$$

where *s* is the equivalent factor, and Q_{lhv} is the low heating value of fuel. The driving cycles to optimize the mentioned parameters are derived from the collected driving data including different driving behaviours presented in [45]. During optimization, the subjected constraints can be summarized, as:

$$\begin{cases} SOC_{min} \le SOC \le SOC_{max} \\ P_{batt\_min} \le P_{batt} \le P_{batt\_max} \\ T_{em\_min} \le T_{em} \le T_{em\_max} \\ \omega_{em\_min} \le \omega_{em} \le \omega_{em\_max} \\ v_{min} \le v \le v_{max} \\ \dot{v}_{min} \le \dot{v} \le \dot{v}_{max} \end{cases} \tag{37}$$

where the maximum and minimum velocities and accelerations for different driving behaviours are defined based on the calculated average maximum and minimum values of the collected driving data for DBI training.

BASED ON THE INNOVATIVE DESIGN, A NOVEL TORQUE DEMAND REGULATION METHOD IS OBTAINED TO FACILITATE ECO-DRIVING UNDER DIFFERENT DRIVING BEHAVIOURS. THE NOVEL TORQUE DEMAND REGULATION METHOD PRESENTS AN EFFICIENT MANNER FOR THE CONTROL DEVELOPMENT OF EV, AND FURTHER EXCAVATES THE POTENTIAL OF EVS WITH SPD IN ECO-DRIVING. IN ADDITION, THE BRAND-NEW DBI ACCELERATES THE DESIGN OF NEW VEHICLE-DRIVER COOPERATIVE CONTROL METHODS FOR PROMOTING ENERGY CONSUMPTION ECONOMY, AND THE PROPOSED TORQUE DEMAND REGULATION METHOD CAN BE EASILY TRANSPLANTED TO DIFFERENT EVS BY ADJUSTING THE PARAMETERS DETAILED IN (1) TO (6) AND CONSTRAINTS PRESENTED IN (36) AND (37), THUS MITIGATING THE APPLICATION DIFFICULTY FOR DIFFERENT TYPES OF EVS.

IV. DRIVING BEHAVIOR CLASSIFICATION AND CASE STUDY

4.1 Assessment on ANFIS-PSO Based Driving Behavior Classification

As described previously, the novel torque demand regulation method cannot be applied properly without precise driving behaviour identification. The ANFIS-PSO based driving behaviour classifier is assessed before performing further evaluation, and the detailed introduction can be referred to our former work [45]. The self-report questionnaire based quantitative analysis is applied firstly to cluster 50 drivers into three groups that are corresponding to the defined driving behaviours [6]. Then, 30 drivers belonging to different groups are requested to drive the vehicle on a fixed route that combines city and highway driving condition, as shown in Fig. 5. The corresponding data selected by the BDA is collected to train the ANFIS-PSO. Afterwards, 20

drivers from three groups with various driving behaviours are requested to drive the vehicle on the same route. The collected data from 20 drivers, which is instructed by the BDA and labelled with disperse driving behaviours, is implemented to test the ANFIS-PSO based identifier. Table 5 lists the numerical identification results of the test, during which the ANFIS-PSO based identifier can classify different driving behaviours with 1 or 2 misrecognitions in each case. The classification on Eco-Pro behaviour shows major malfunctions. This is because the close performance between Eco-Pro and Normal typed drivers happens in some driving conditions. Despite minor errors, the general performance of ANFIS-PSO based identifier can still support the applications of the novel torque demand regulation method.

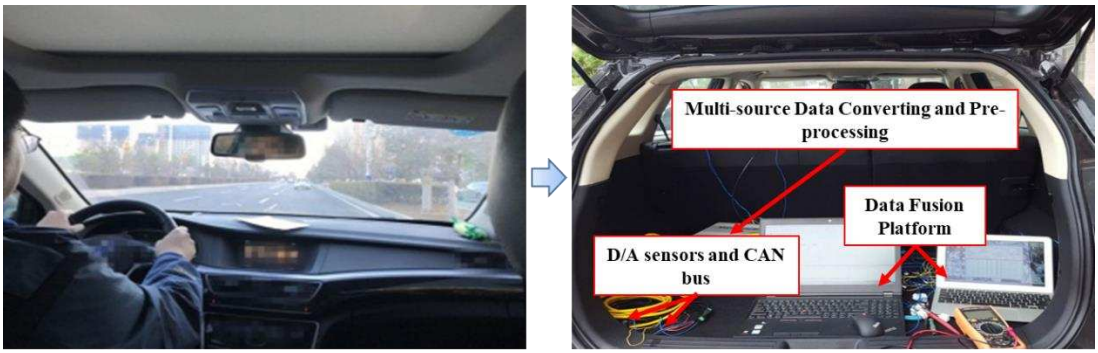

Fig. 5. Route test for data collection.

Table 5. Results of driving behaviour identification under different driving behaviours.

Driving Behavior Type	Number of Driver in Test	Number of Rightly Identified Driver
Expert-Pro	3	2
Normal	12	11
Eco-Pro	5	3

4.2 Case Study on Performance of Novel Method in Eco-driving

The presented torque demand method can generate TDLTs for disperse driving behaviors, thereby broadening the scope of eco-driving exhaustively. A case study is performed to validate the performance of the proposed method, and define critical roles of driving behaviors in eco-driving. In this special case study, the generated TDLTs by the introduced method are integrated into velocity profile optimization for EV operation. The optimal velocity profile for efficient driving, on the basis of certain TDLT, is yielded by dynamic programming (DP) [46].

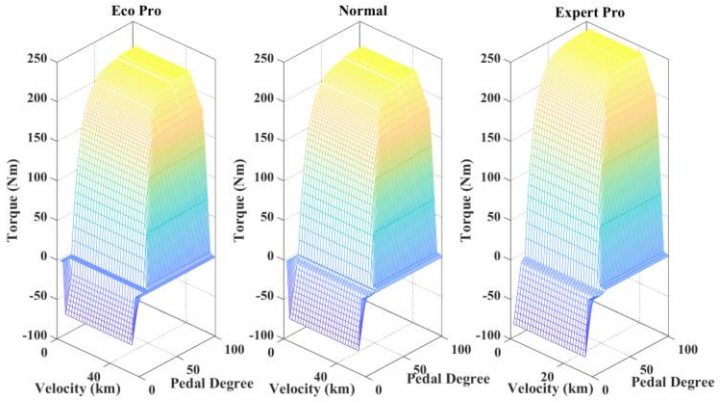

Fig. 6. 3D TDLTs for different driving behaviours.

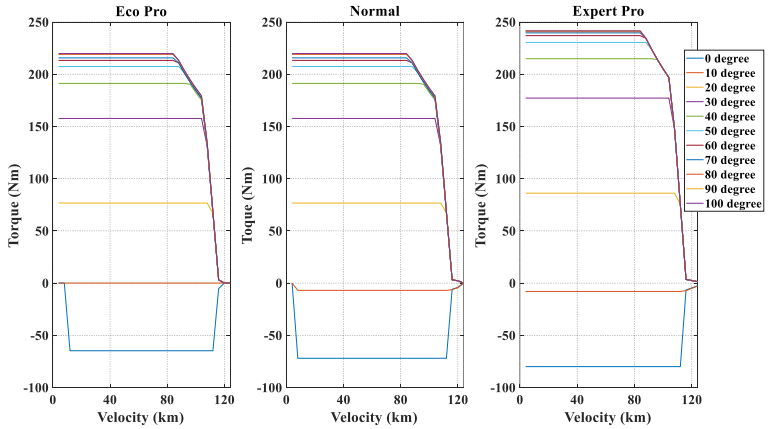

Fig. 7. 2D TDLTs for different driving behaviours.

For the velocity profile optimization problem, the cost function at step k can be formulated, as:

$$J_k(x^i)=\left\{h_k(x_k^i,u_k^j)+J_{k+1}\left(F_k(x_k^i,u_k^j)\right)\right\}=\left\{L_k(v_k^i,T_{mot\_k}^j)+J_{k+1}(F_k(v_k^i,T_{mot\_k}^j)\right\} \tag{38}$$

where the state variable is velocity, and the required tractive torque by motor T_{mot} is obtained via interpolating the implemented TDLT after referring to the given acceleration pedal degree, which is defined as the control variable. The particular stage cost can be formulated, as:

$$L_k(x_k^i,u_k^j)=L_k(v_k^i,T_k^j)=\omega_t\cdot\frac{2\cdot P_{batt}(v_k^i,T_{mot\_k}^j)\cdot\Delta s}{v(k)+v(k+1)}+T_{brk}(v_k^i,T_{mot\_k}^j) \tag{39}$$

where Δs means the step length, and ω_t expresses the weight ratio. For ease of comparison, the optimization is performed in distance domain. Thus, the functions to describe state dynamics should be reformulated. The relationship between speed and location can be formulated, as:

$$v(k+1)=v(k)+\dot{v}(k)\frac{2\Delta s}{v(k)+v(k+1)} \tag{40}$$

where Δs means the calculation step in distance, k and $k+1$ express the location at current and next steps. By combining (40) and (1), the dynamic relationship between motor torque and vehicle speed in distance domain can be derived, as:

$$v(k+1)^2 = (1-\frac{2\Delta s}{m}P_2)v(k)^2 + \frac{2\Delta s}{m}P_1 T_{mot}(k) - \frac{2\Delta s}{m}\frac{T_{brk}}{r_w} - \frac{2\Delta s}{m}P_3 \tag{41}$$

Then, Eqn. (41) can be rewritten into:

$$v(k+1)^2 = \mathrm{A}v(k)^2 + BT_{mot}(k) - CT_{brk} - \mathrm{D} \tag{42}$$

where $A = 1-\frac{\Delta s}{m}\rho C_d A_d$, $B = \frac{2\Delta s g_{fr} N_{fr}}{m r_w}$, $C = \frac{2\Delta s}{m r_w}$, and $D = \frac{2\Delta s}{m}\left(mgfcos\theta(k) + mgsin\theta(k)\right)$. The inequality constraints that the DP based velocity profile optimization should be subject to the same constraints as those in (37). The installed TDLTs generated by the presented method are shown in Figs. 6 and 7, respectively. As can be found, the torque outputs by different driving behaviors are disparate. The TDLT for Expert Pro behavior tends to provide larger tractive torque, and the utilization of freewheeling is quite rare. Nonetheless, the TDLT for Eco Pro behavior tries to employ both the freewheeling and electric braking in SPD cooperatively, contributing to energy saving. Moreover, the TDLT for normal behavior evenly balance the energy-saving and drivability, showing promising performance either.

Fig. 8 exhibits the optimized velocity profiles after applying different TDLTs. Except the optimal velocity profile, the velocity profile collected from real driving is shown and named as Raw in Fig. 8. The zoomed-in graphs of velocity profiles are also provided to better understand the difference in velocity profile optimization by different TDLTs. As can be found, the Expert Pro driving behavior prefers to drive the vehicle more aggressively with higher and more frequent acceleration and deceleration. The freewheeling by Expert Pro behavior seldom occurs in the optimized velocity profile. The TDLT for normal driving attains the close top speeds to those by the Expert-Pro based TDLT. The deceleration, dissimilarly, looks smoother, as marked in the velocity profile at around 2150 m and 4150 m. The velocity profile optimized by the TDLT for Eco-Pro behavior is most gentle, and with the least top speeds and deceleration. The freewheeling by Eco-Pro TDLT is actively encouraged for energy saving. Table 6 lists the numerical results during the velocity optimization by DP with different TDLTs, which include the conventional TDLT without any pre-optimization. The DP based optimization with conventional TDLT is denoted as DP_Conventional in Table 6. The numerical results

highlight that the raised method, together with DP, can prompt energy consumption economy under different driving behaviors. Compared with the velocity profile without any optimization, the DP based velocity profile optimization with ingeniously generated TDLTs can save the energy consumption by up to 18.3%. Due to the uncontrolled search manners, the terminal velocity by DP under three driving behaviors cannot reach to zero. However, the unsatisfied terminal velocities will not discredit the capability of the raised method implemented in real control. Additionally, the travel time by DP with Expert-Pro TDLT is less than that with normal TDLT without any optimization. Shorter travel duration is raised by the specially generated TDLT, in which the optimal knowledge of drivability under Expert-Pro driving has been fully taken into consideration. The comparisons among DP based optimization with diverse TDLTs validate the preferable performance of the novel torque demand regulation method. Under any driving behaviors, the given TDLT can instruct the most appropriate torque output with roundly incorporating the knowledge from eco-driving and drivability by WOA. In comparison with optimization with conventional TDLT, the proposed method can facilitate the DP based optimization to furnish energy saving by up to 13.3%.

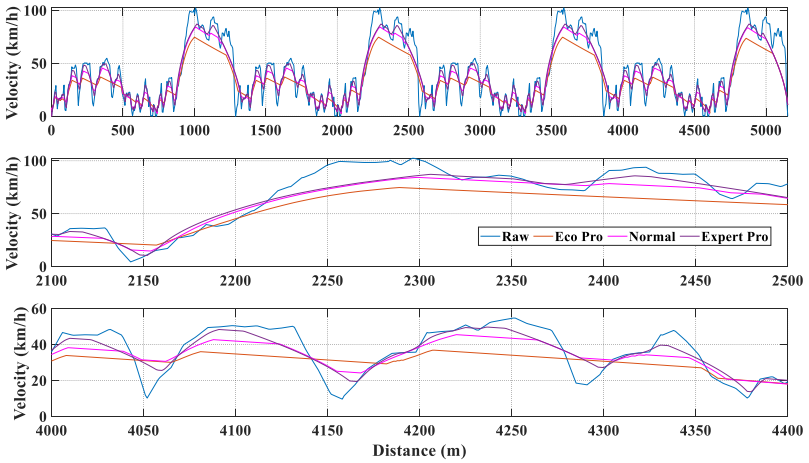

Fig. 8. Optimal velocity profiles under different driving behaviours.

Figs. 9 and 10 illustrate the pedal degrees and motor torques by DP with different TDLTs in the case study. In Fig. 9, the acceleration pedal degrees are represented by the values that are larger than 0, and the braking pedal degrees means the values that are smaller than 0. As can be found, the motor torques by DP with different TDLTs highlight obvious difference. The TDLT for the Expert-Pro behavior requires larger motor torques than other two TDLTs. The TDLT for the Eco-Pro behavior regulates the motor to output tractive force more mildly than other two TDLTs. The acceleration pedal also joins in the braking process in EV with SPD. The optimal TDLTs decelerate the vehicle in various manners. The TDLT for the Expert-Pro behavior is prone

to heavy brake without seeking assistance from freewheeling. The TDLT for the Eco-Pro behavior encourages united employment of electric braking from SPD, mechanical braking from braking pedal and freewheeling, thereby manipulating the vehicle more moderately. Fig. 11 shows the motor operation points under different behaviors during the velocity profile optimization. The WOA based pre-optimization endows TDLTs with optimal knowledge of eco-driving, and facilitates the motor to operate in efficient fields under different driving behaviors.

Table 6. Numerical results during velocity prediction by DP with different TDLTs.

Method	n_x	n_u	Δs (m)	s_t (m)	*Ini_v* (m/s)	*Ter_v* (m/s)	*E_con* (kWh)	*T_tol* (s)
DP_Eco Pro	200	200	2	5152	0	1.9712	0.4016	453.221
DP_Normal	200	200	2	5152	0	1.9731	0.4239	426.105
DP_Expert Pro	200	200	2	5152	0	1.9723	0.4513	387.368
DP_Covention al	200	200	2	5152	0	1.9716	0.4632	389.477
Raw	-	-	-	5152	0	0	0.4913	392.136

Note that n_x and n_u are the number of discrete state and control variables in each step, Δs is the simulation step, s_t it the total travel distance, *Ini_v* and *Ter_v* are the initial speed and target speed, *E_con* is the energy consumption on the route, and *T_tol* is the travel time on the route.

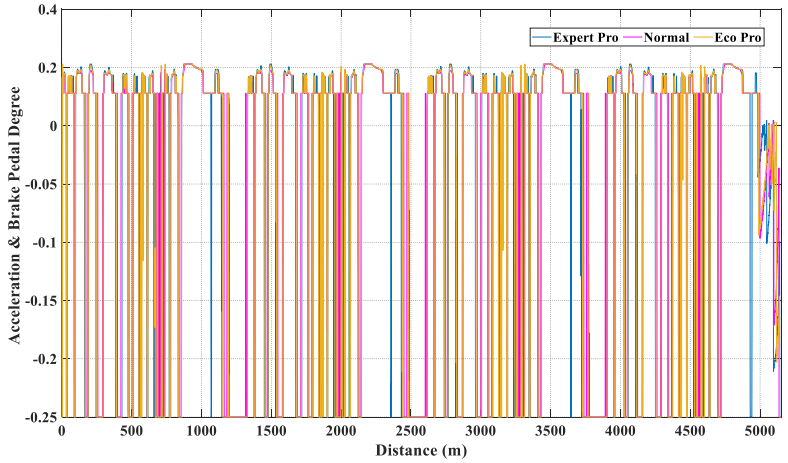

Fig. 9. Pedal degrees under different driving behaviours in velocity profile optimization.

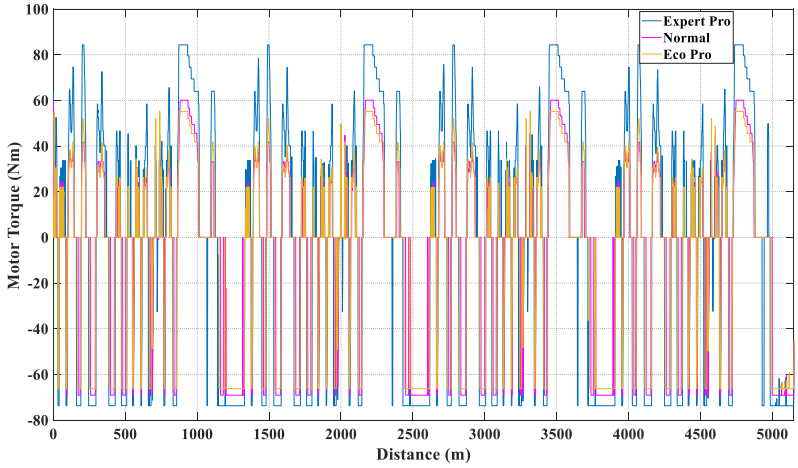

Fig. 10. Motor torque under different driving behaviours in velocity profile optimization.

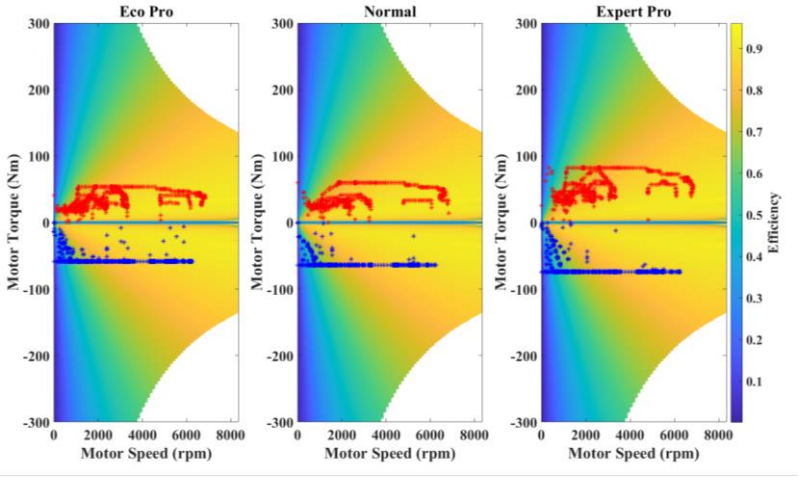

Fig. 11. Motor operation points under different driving behaviours in velocity profile optimization.

According to the results of the case study, it can be summarized that the driving behaviors impose distinctive impact on efficient driving. Further, drivers prefer to manipulate vehicles with different manners. Some eco maneuver e.g. freewheeling might by adopted by drivers, which is quite valuable for energy saving. Some aggressive behaviors, e.g. sudden heavy acceleration, may deteriorate driving economy. As the dominate factor in efficient driving, driving behaviors should be involved in vehicle control. The raised method can rationally enrich the normal TDLT with driving behavior information, thereby obtaining qualified performance. Through the evaluation and case study, the proposed novel torque demand method demonstrates the superior capability in prompting eco-driving for EV with SPD under different driving conditions. The gratifying performance derives from the ANFIS-PSO and BDA based driving behaviors classification and WOA based TDLT optimization. The cooperation of driving behavior classification and TDLT optimization successfully integrates the driver and optimization knowledge into vehicle control, strengthening better energy economy without discounting the drivability.

V. CONCLUSION

This paper develops a novel torque demand regulation method for electric vehicle with single pedal driving, and the method promotes efficient driving under different driving behaviors. A specific torque demand look-up table, corresponding to the identified driving behavior, is implemented in vehicle control unit to generate the optimal tractive torque for next step energy-saving traction control. The instant driving behavior classifier is constructed by virtue of the adaptive neuro fuzzy inference system with particle swarm optimization. The binary dragonfly algorithm is exploited to select valuable features as the inputs of the built

driving behavior classifier, thereby enhancing the accuracy of driving behavior categorization. Given the particular constraints under certain driving behavior, the whale optimization algorithm is employed to optimally generate the specific torque demand look-up table offline. With the driving behavior oriented optimization, the energy economy of the studied electric vehicle is improved dramatically. The case study results manifest the promising impact of the proposed torque demand regulation method in optimal control for eco-driving. By incorporating the optimized torque demand look-up tables, the energy consumption of the studied vehicle in traction optimization has been reduced significantly under all driving behaviors. In particular, the electricity consumed under Eco-Pro behaviors occupies only 86.7 % of that with the conventional torque demand look-up table, and compared with that by the conventional torque demand look-up table without any optimization, the electricity consumption under Normal and Expert-Pro behaviors is respectively saved by 8.5% and 2.6%, manifesting the qualified performance of the proposed algorithm.

In the future, more effort will be devoted to studies related to intelligent single pedal driving. The combined optimization on driving comfort, safety and energy efficiency will be investigated by applying advanced control methods. Additionally, deep learning methods to identify driving behaviors incorporating facial emotion, maneuver gestured and manipulating signals will be carefully investigated.

ACKNOWLEDGEMENT

This work was supported in part by the National Natural Science Foundation of China (No. 61763021 and 51775063), in part by the EU-funded projects MODALES (No. 815189), PAsCAL (No. 815098) and ELVITEN (No. 769926) and in part by the EU-funded Marie Skłodowska-Curie Individual Fellowships Project (No. 845102).

REFERENCE

[1] Ferro, G., R. Minciardi, and M. Robba. "A user equilibrium model for electric vehicles: Joint traffic and energy demand assignment." Energy (2020): 117299.
[2] Tao, Ye, et al. "Orderly charging strategy of battery electric vehicle driven by real-world driving data." Energy 193 (2020): 116806.
[3] Rezaei, Navid, et al. "Economic energy and reserve management of renewable-based microgrids in the presence of electric vehicle aggregators: A robust optimization approach." Energy (2020): 117629.
[4] Zhang, Fengqi, et al. "Adaptive energy management in automated hybrid electric vehicles with flexible torque request." Energy 214 (2020): 118873.
[5] Olabi, A. G., Tabbi Wilberforce, and Mohammad Ali Abdelkareem. "Fuel cell application in the automotive industry and future perspective." Energy 214 (2020): 118955.
[6] X. F. Ding et al., "Analytical and Experimental Evaluation of SiC-Inverter Nonlinearities for Traction Drives Used in Electric Vehicles," IEEE Transactions on Vehicular Technology, Article vol. 67, no. 1, pp. 146-159, Jan 2018.
[7] Zhang, Youlang, et al. "Performance assessment of retired EV battery modules for echelon use." Energy 193 (2020): 116555.

[8] N. Ding, K. Prasad, and T. T. Lie, "Design of a hybrid energy management system using designedrule-basedcontrol strategy and genetic algorithm for the series-parallel plug-in hybrid electric vehicle," International Journal of Energy Research, 2020.
[9] F. Q. Zhang, X. S. Hu, R. Langari, and D. P. Cao, "Energy management strategies of connected HEVs and PHEVs: Recent progress and outlook," Progress in Energy and Combustion Science, Review vol. 73, pp. 235-256, Jul 2019.
[10] F. T. Zhang, F. Y. Yang, D. L. Xue, and Y. C. Cai, "Optimization of compound power split configurations in PHEV bus for fuel consumption and battery degradation decreasing," Energy, Article vol. 169, pp. 937-957, Feb 2019.
[11] C. Yang, S. X. You, W. D. Wang, L. Li, and C. L. Xiang, "A Stochastic Predictive Energy Management Strategy for Plug-in Hybrid Electric Vehicles Based on Fast Rolling Optimization," IEEE Transactions on Industrial Electronics, Article vol. 67, no. 11, pp. 9659-9670, Nov 2020.
[12] J. Q. Guo, H. W. He, J. K. Peng, and N. N. Zhou, "A novel MPC-based adaptive energy management strategy in plug-in hybrid electric vehicles," Energy, Article vol. 175, pp. 378-392, May 2019.
[13] J. Li, Y. Liu, D. Qin, G. Li, and Z. Chen, "Research on Equivalent Factor Boundary of Equivalent Consumption Minimization Strategy for PHEVs," IEEE Transactions on Vehicular Technology, vol. 69, no. 6, pp. 6011-6024, Jun 2020.
[14] Q. Zhang, K. Wu, and Y. Shi, "Route Planning and Power Management for PHEVs With Reinforcement Learning," IEEE Transactions on Vehicular Technology, vol. 69, no. 5, pp. 4751-4762, May 2020.
[15] X. W. Qi, Y. D. Luo, G. Y. Wu, K. Boriboonsomsin, and M. Barth, "Deep reinforcement learning enabled self-learning control for energy efficient driving," Transportation Research Part C-Emerging Technologies, Article vol. 99, pp. 67-81, Feb 2019.
[16] A. Aksjonov, V. Ricciardi, K. Augsburg, V. Vodovozov, and E. Petlenkov, "Hardware-in-the-Loop Test of an Open Loop Fuzzy Control Method for Decoupled Electro-Hydraulic Antilock Braking System," IEEE Transactions on Fuzzy Systems, pp. 1-1, 2020.
[17] Y. Yuan and J. Z. Zhang, "A Novel Initiative Braking System With Nondegraded Fallback Level for ADAS and Autonomous Driving," IEEE Transactions on Industrial Electronics, Article vol. 67, no. 6, pp. 4360-4370, Jun 2020.
[18] S. A. Sajadi-Alamdari, H. Voos, and M. Darouach, "Nonlinear Model Predictive Control for Ecological Driver Assistance Systems in Electric Vehicles," Robotics and Autonomous Systems, Article vol. 112, pp. 291-303, Feb 2019.
[19] M. Khanra and A. K. Nandi, "Optimal driving based trip planning of electric vehicles using evolutionary algorithms: A driving assistance system," Applied Soft Computing, vol. 93, Aug 2020, Art. no. 106361.
[20] Y. Saito, P. Raksincharoensak, and Ieee, "Risk Predictive Haptic Guidance: Driver Assistance with One-pedal Speed Control Interface," in 2017 IEEE International Conference on Systems, Man, and Cybernetics(IEEE International Conference on Systems Man and Cybernetics Conference Proceedings, 2017, pp. 111-116.
[21] W. Liu, H. Z. Qi, X. T. Liu, and Y. S. Wang, "Evaluation of regenerative braking based on single-pedal control for electric vehicles," Frontiers of Mechanical Engineering, Article vol. 15, no. 1, pp. 166-179, Mar 2020.
[22] H. W. He, C. Wang, H. Jia, and X. Cui, "An intelligent braking system composed single-pedal and multi-objective optimization neural network braking control strategies for electric vehicle," Applied Energy, Article vol. 259, p. 14, Feb 2020, Art. no. 114172.
[23] R. A. Kulas, H. Rieland, and J. Pechauer, "A System Safety Perspective into Chevy Bolt's One Pedal Driving," in WCX SAE World Congress Experience, 2019.
[24] U. Caliskan and V. Patoglu, "Efficacy of Haptic Pedal Feel Compensation on Driving With Regenerative Braking," IEEE Transactions on Haptics, Article vol. 13, no. 1, pp. 175-182, Jan-Mar 2020.
[25] Yongqiang, Zhao, et al. "A research on evaluation and development of single-pedal function for electric vehicle based on PID." Journal of Physics: Conference Series. Vol. 1605. No. 1. IOP Publishing, 2020.
[26] Van Boekel, J. J. P., I. J. M. Besselink, and Henk Nijmeijer. "Design and realization of a One-Pedal-Driving algorithm for the TU/e Lupo EL." World Electric Vehicle Journal 7.2 (2015): 226-237.
[27] Wen, He Hong, Wang Chen, and Jia Hui. "A single-pedal regenerative braking control strategy of accelerator pedal for electric vehicles based on adaptive fuzzy control algorithm." Energy Procedia 152 (2018): 624-629.
[28] Ji, Fenzhu, et al. "Energy recovery based on pedal situation for regenerative braking system of electric vehicle." Vehicle system dynamics 58.1 (2020): 144-173.
[29] D. Shinar, E. Schechtman, and R. Compton, "Self-reports of safe driving behaviors in relationship to sex, age, education and income in the US adult driving population," Accident; analysis and prevention, vol. 33, no. 1, pp. 111-6, 2001-Jan 2001.
[30] C. Fullwood, S. Quinn, L. K. Kaye, and C. Redding, "My virtual friend: A qualitative analysis of the attitudes and experiences of Smartphone users: Implications for Smartphone attachment," Computers in Human Behavior, Article vol. 75, pp. 347-355, Oct 2017.
[31] L. Liao et al., "Hierarchical quantitative analysis to evaluate unsafe driving behaviour from massive trajectory data," Iet Intelligent Transport Systems, vol. 14, no. 8, pp. 849-856, Aug 2020.
[32] Y. Xing, C. Lv, Y. Zhao, Y. Liu, D. Cao, and S. Kawahara, "Pattern Recognition and Characterization of Upper Limb Neuromuscular Dynamics during Driver-Vehicle Interactions," Iscience, vol. 23, no. 9, Sep 25 2020.

[33] P. Hang, C. Lv, Y. Xing, C. Huang, and Z. Hu, "Human-Like Decision Making for Autonomous Driving: A Noncooperative Game Theoretic Approach," 2020.
[34] O. A. Osman, M. Hajij, S. Karbalaieali, and S. Ishak, "A hierarchical machine learning classification approach for secondary task identification from observed driving behavior data," Accident Analysis and Prevention, Article vol. 123, pp. 274-281, Feb 2019.
[35] H. L. Liu, T. Taniguchi, Y. Tanaka, K. Takenaka, and T. Bando, "Visualization of Driving Behavior Based on Hidden Feature Extraction by Using Deep Learning," IEEE Transactions on Intelligent Transportation Systems, Article vol. 18, no. 9, pp. 2477-2489, Sep 2017.
[36] W. Zhou, L. Yang, Y. Cai, and T. Ying, "Dynamic programming for New Energy Vehicles based on their work modes part I: Electric Vehicles and Hybrid Electric Vehicles," Journal of Power Sources, vol. 406, pp. 151-166, Dec 1 2018.
[37] C. M. Martinez, X. Hu, D. Cao, E. Velenis, B. Gao, and M. Wellers, "Energy Management in Plug-in Hybrid Electric Vehicles: Recent Progress and a Connected Vehicles Perspective," IEEE Transactions on Vehicular Technology, vol. 66, no. 6, pp. 4534-4549, Jun 2017.
[38] G. Rizzoni, L. Guzzella, and B. M. Baumann, "Unified modeling of hybrid electric vehicle drivetrains," IEEE/ASME Transactions on Mechatronics, vol. 4, no. 3, pp. 246-257, Sep 1999.
[39] C. C. Lin, H. Peng, J. W. Grizzle, and J. M. Kang, "Power management strategy for a parallel hybrid electric truck," IEEE Transactions on Control Systems Technology, vol. 11, no. 6, pp. 839-849, Nov 2003.
[40] T. Z. Zhang, S. Liu, C. S. Xu, B. Liu, and M. H. Yang, "Correlation Particle Filter for Visual Tracking," IEEE Transactions on Image Processing, Article vol. 27, no. 6, pp. 2676-2687, Jun 2018.
[41] P. A. Adedeji, S. Akinlabi, N. Madushele, and O. O. J. I. J. o. A. E. Olatunji, "Hybrid Adaptive Neuro-fuzzy Inference System (ANFIS) for a Multi-campus University Energy Consumption Forecast," pp. 1-20, 2020.
[42] M. Petrovic, V. Rakocevic, N. Kontrec, S. Panic, and D. Ilic, "Hybridization of accelerated gradient descent method," Numerical Algorithms, vol. 79, no. 3, pp. 769-786, Nov 2018.
[43] Q. Wang et al., "Regularized moving least-square method and regularized improved interpolating moving least-square method with nonsingular moment matrices," Applied Mathematics and Computation, vol. 325, pp. 120-145, May 15 2018.
[44] Y. M. Ding, W. L. Zhang, L. Yu, and K. H. Lu, "The accuracy and efficiency of GA and PSO optimization schemes on estimating reaction kinetic parameters of biomass pyrolysis," Energy, Article vol. 176, pp. 582-588, Jun 2019.
[45] Y. J. Zhang et al., "Optimal energy management strategy for parallel plug-in hybrid electric vehicle based on driving behavior analysis and real time traffic information prediction," Mechatronics, Article vol. 46, pp. 177-192, Oct 2017.
[46] A. I. Hammouri, M. Mafarja, M. A. Al-Betar, M. A. Awadallah, and I. Abu-Doush, "An improved Dragonfly Algorithm for feature selection," Knowledge-Based Systems, Article vol. 203, p. 16, Sep 2020, Art. no. 106131.
[47] L. L. Li, X. Zhao, M. L. Tseng, and R. R. Tan, "Short-term wind power forecasting based on support vector machine with improved dragonfly algorithm," Journal of Cleaner Production, Article vol. 242, p. 12, Jan 2020, Art. no. 118447.
[48] R. Sawhney and R. Jain, "Modified Binary Dragonfly Algorithm for Feature Selection in Human Papillomavirus-Mediated Disease Treatment," in 2018 International Conference on Communication, Computing and Internet of Things (IC3IoT), 2018, pp. 91-95.
[49] S. Mirjalili and A. Lewis, "The Whale Optimization Algorithm," Advances in Engineering Software, Article vol. 95, pp. 51-67, May 2016.
[50] I. Aljarah, H. Faris, and S. Mirjalili, "Optimizing connection weights in neural networks using the whale optimization algorithm," Soft Computing, Article vol. 22, no. 1, pp. 1-15, Jan 2018.
[51] Y. T. Zhou et al., "Hybrid genetic algorithm method for efficient and robust evaluation of remaining useful life of supercapacitors," Applied Energy, Article vol. 260, p. 15, Feb 2020, Art. no. 114169.